Research Article | Vol. 25, No. 22 | 30 Oct 2017 | OPTICS EXPRESS 27750
Optics EXPRESS

DFT/IDFT-free receiving scheme for spread-OFDM signals employing low-sampling-rate ADCs

CHI-HSIANG LIN,[1] CHUN-TING LIN,[1,*] CHIA-CHIEN WEI,[2] AND SIEN CHI[1]

[1]*Institute of Photonic System, National Chiao Tung University, Tainan, Taiwan*
[2]*Department of Photonics, National Sun Yat-sen University, Kaohsiung, Taiwan*
[*]*jinting@mail.nctu.edu.tw*

Abstract: This paper presents a DFT/IDFT-free receiving scheme for spread-OFDM signals. Leveraging sub-Nyquist sampling and proper sampling delay, the proposed scheme enables each user to receive the requested data without the need for DFT and IDFT; thus, the complexity at receiver can be greatly reduced. Nonetheless, DC component is altered in an AC coupling system, such that severe waveform distortion is caused when the process of DFT/IDFT is omitted. Thus, a DC-zeroing algorithm is proposed to guarantee constant DC after sub-Nyquist sampling, thereby eliminating such distortion. To experimentally verify the concept of proposed scheme, a 27.15-Gbit/s optical spread-OFDM signal was transmitted over fiber and received by the DFT/IDFT-free scheme with sub-Nyquist sampling. More users will reduce the required sampling rate at receiver; for the case of 16 users, the required sampling rate for the 27.15-Gbit/s signal is as low as 1 GSample/s. The experimental results show that error-free transmission was achievable, and the penalty due to lowering sampling rate (i.e., increasing the number of users) is insignificant.

OCIS codes: (060.2330) Fiber optics communications; (060.4254) Networks, combinatorial network design.

References and links

1. R. Prasad and T. Ojanpera, "A survey on CDMA: evolution towards wideband CDMA," in *International Symposium on Spread Spectrum Techniques and Applications – Proceedings* (IEEE, 1998), pp.323–331.
2. R. Costa, P. Portugal, F. Vasques, and R. Moraes, "A TDMA-based mechanism for real-time communication in IEEE 802.11e networks," in *Conference on Emerging Technologies & Factory Automation* (IEEE, 2010), pp. 1–9.
3. C. Ciochina and H. Sari, "A review of OFDMA and single-carrier FDMA," in *European Wireless Conference* (IEEE, 2010), pp. 706–710.
4. E. Yaacoub and Z. Dawy, "A Survey on Uplink Resource Allocation in OFDMA Wireless Networks," Communications Surveys & Tutorials **14**(2), 322–337 (2012).
5. Y. m. Lin and P. l. Tien, "Next-generation OFDMA-based passive optical network architecture supporting radio-over-fiber," J. Sel. Areas Commun. **28**(6), 791–799 (2010).
6. T. Jiang and Y. Wu, "An Overview: Peak-to-Average Power Ratio Reduction Techniques for OFDM Signals," Transactions on Broadcasting **54**(2), 257–268 (2008).
7. H. G. Myung, "Introduction to single carrier FDMA," in *European Signal Processing Conference* (IEEE, 2007), pp. 2144–2148.
8. X. Han, N. Zhao, Q. Wei, F. Qiao, H. Yang, and H. Wang, "A single channel, 6-bit 410-ms/s asynchronous SAR ADC based on 3bits/stage," in *International New Circuits and Systems Conference* (IEEE, 2014), pp. 57–60.
9. A. Hekimyan, D. Bulakh, and A. Sahakyan, "High accuracy pipelined ADC design for wireless LANs," in *Internet Technologies and Applications* (IEEE, 2015), pp. 312–314.
10. C. C. Wei, H. C. Liu, C. T. Lin, and S. Chi, "Analog-to-Digital Conversion Using Sub-Nyquist Sampling Rate in Flexible Delay-Division Multiplexing OFDMA PONs," in J. of Lightwave Techno. **34**(10), 2381–2390 (2016).

1. Introduction

Recently, considerable research in the field of communication has been focused on supporting multiuser system [1–7]. In particular, these techniques usually fall under the down-link environment, which allows reducing the interference between users and simplify hardware architecture. Conventionally, the communication between the base station (BS) and the users is based on orthogonal multiple-access channel (MAC), such as code domain division, time

#301067 https://doi.org/10.1364/OE.25.027750
Journal © 2017 Received 30 Jun 2017; revised 27 Sep 2017; accepted 15 Oct 2017; published 26 Oct 2017

Optics EXPRESS

domain division, and frequency domain division [1–3]. As a kind of frequency domain division, orthogonal frequency division multiplexing access (OFDMA) is widely utilized in current communication system (e.g., Long Term Evolution, Wi-Fi, OFDM Passive Optical Network, etc.) and especially in the down-link stream [4, 5]. This method has been extended to investigate with quadrature-amplitude modulation (QAM), which can achieve higher data rate for supporting each user. However, OFDMA with QAM modulation suffer from a high peak-to-average-power ratio (PAPR) and demand stricter requirements pertaining to digital-to-analog converters (DACs)/analog-to-digital converters (ADCs) [6]. Meanwhile, spread-OFDM was developed to reduce PAPR; however, high computational complexity from discrete Fourier transform (DFT)/ inverse discrete Fourier transform (IDFT) at receiver inhibits this method in down-link applications [7]. In particular, each user in a multiuser system needs to process high-speed aggregated spread-OFDM/OFDM data for receiving only a small portion of data. On the other hand, even though high sampling-rate (SR) ADCs and interleaved low SR ADCs are widely used and developed at the receiver, as shown in Fig. 1(a) and 1(b), respectively, they are still difficult to design and not cost-effective for users in a high-speed spread-OFDM/OFDM system. More recently, to relax the requirements of ADCs, we proposed delay-division-multiplexing (DDM) scheme to enable the formulation of OFDM featuring a sub-Nyquist sampling rate ADC [8–10], but DFT is still needed for OFDM demodulation.

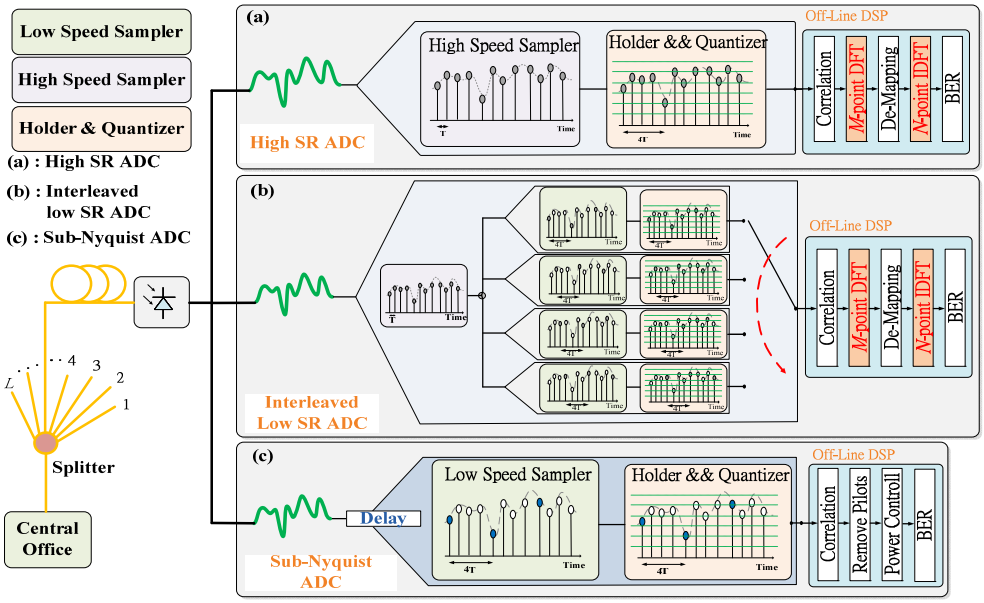

Fig. 1. Schematic diagrams of different receiving architectures.

In order to satisfy the future multiuser down-link data traffic, this paper presents a pre-processing method for spread-OFDM, which is capable of eliminating aliasing from receiving high-speed aggregated data using single sub-Nyquist ADC, as shown in Fig. 1(c). The proposed pre-processing method reduces the sampling rate of the ADC to 1/*L* of the Nyquist sampling rate while eliminating the need for DFT/IDFT at the receiver, where *L* is the number of users. This approach greatly reduces the computational complexity of spread-OFDM application, thereby making it suitable for down-link streaming. However, signal distortion is caused by removing DC component in an AC coupling system when the process of DFT/IDFT is omitted. Consequently, a DC-zeroing algorithm is also proposed to guarantee constant DC component after sub-Nyquist sampling, which thereby eliminates DC distortion. To experimentally verify the concept of proposed scheme, a 27.15-Gbit/s optical spread

Optics EXPRESS

OFDM signal was demonstrated for supporting 16 users, wherein each user receives their data stream via DFT/IDFT-free receiver with a 1-GSample/s ADC (i.e. sampling rate reduction is up to 1/16).

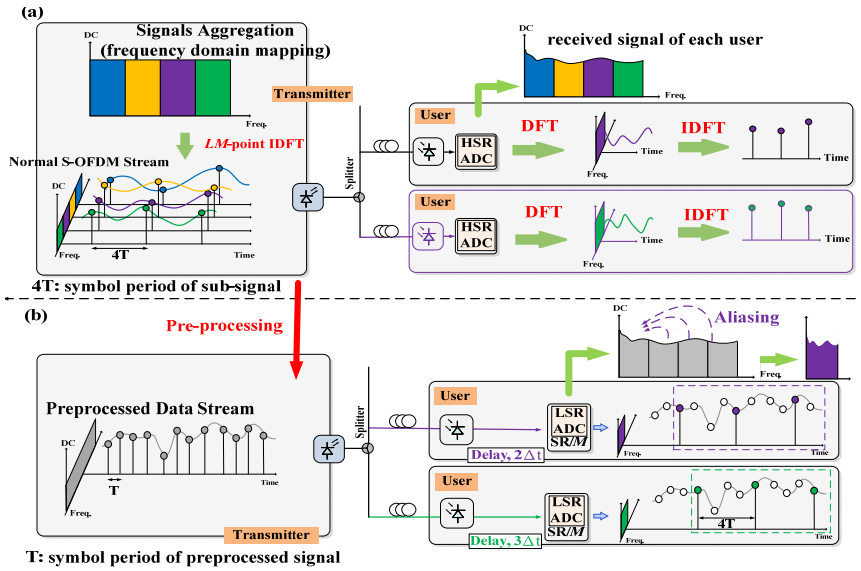

Fig. 2. Architectures of (a) 4-user traditional spread-OFDM system and (b) 4-user proposed spread-OFDM system.

2. Concept

Figure 2(a) presents the architecture of traditional spread-OFDM system. Frequency-domain mapping is necessary at transmitter to aggregate down-link signals, and a user needs to de-map the received signal through DFT/IDFT, before acquiring the desired time-domain signal. In should be noted that the received signal must be sampled by an ADC at a rate faster than the Nyquist rate, such that the following DFT can separate the desired spectrum from the others. Moreover, Fig. 2(b) schematically plots the concept of proposed sub-Nyquist receiving scheme for a spread-OFDM system. Enabled by proper pre-processing at the transmitter [10], the proposed scheme leverages intentional aliasing by sub-Nyquist sampling to directly receive the desired signal without de-mapping and DFT/IDFT. Different users can obtain different data by setting different initial sampling instants, as indicated in Fig. 2(b) and detailed in [10]. Thus, through lowering the sampling rate and omitting DFT/IDFT, the proposed scheme can significantly reduce the complexity of receiver, compared to the traditional scheme.

However, unlike OFDM using sub-Nyquist sampling in [10], spread-OFDM encodes data in time domain. Considering down-link spread-OFDM for L users, a time-domain signal sent to the l^{th} user with N-point DFT block can be represented as a complex vector $\mathbf{s}_l = [\, s_{(l-1)N+1} \;\; s_{(l-1)N+2} \cdots \; s_{lN} \,]^{\mathrm{T}}$. After DFT at transmitter, frequency-domain information of $\mathbf{s}_l$ is written as $\mathbf{x}_l = [\, x_{(l-1)N+1} \;\; x_{(l-1)N+2} \ldots x_{lN} \,]^{\mathrm{T}}$. Since cost-sensitive optical access networks prefer intensity modulation and direct detection (IMDD), the time-domain samples in our discussion must be limited to real-valued; thus, mapped frequency-domain information ($\hat{\mathbf{x}}_l$) must be rearranged as,

$$\hat{\mathbf{x}}_l = [\, x_{(l-1)N+1} \; x_{(l-1)N+2} \ldots x_{lN} \;\; x^*_{(l-1)N+1} \; x^*_{lN} \ldots x^*_{(l-1)N+2} \,]^{\mathrm{T}}, \qquad (1)$$

where * indicates the operation involved in obtaining a complex conjugate. In (1), since $x_{(l-1)N+1}$ represents the DC term in DFT block, $x_{(l-1)N+1} = x^*_{(l-1)N+1}$ is the other requirement to guarantee real-valued time-domain samples. Then, the pre-processing with the knowledge of channel responses, which is detailed in [10], can make the l^{th} user to receive the time-domain signal of $\hat{\mathbf{x}}_l$ directly by sub-Nyquist sampling.

Nonetheless, an AC coupling system will alter the DC term, i.e., the first component in (1), leading to distortion of received waveform. Thus, enforcing the DC term to zero before pre-processing is necessary in avoiding DC-altered distortion in an AC coupling system. It should be noted that this requirement is not required in the sub-Nyquist receiving scheme for OFDM [10] because DFT is applied to acquire the data carried by subcarriers. As shown in Fig. 3, the proposed DC-zeroing scheme is to use the first K symbols in $\mathbf{s}_l$ as pilot symbols, which enforce the average amplitude to zero (i.e., $x_{(l-1)N+1} = \sum_{n=1}^{N} s_{(l-1)N+n} = 0$). Thus, the pilot symbols are defined as follows:

$$s_{(l-1)N+i} = -\frac{1}{K}\sum_{n=K+1}^{N} s_{(l-1)N+n}, \quad i = 1, 2, \ldots, K \tag{2}$$

Overhead associated with the use of pilot symbols is equal to K/N. To compare the performance with two methods, in the simulation, cyclic prefix (CP) was set to 1/32, overhead was set to 4/32, and number of user was set to 16. Without the DC-zeroing algorithm, we remove the quadrature component of DC term (i.e., replacing $x_{(l-1)N+1}$ by $\mathrm{Re}\{x_{(l-1)N+1}\}$) to satisfy $x_{(l-1)N+1}$ being real number. Then, the receiver filters out DC term to prevent AC coupling components from damage (i.e., $\mathrm{Re}\{x_{(l-1)N+1}\}$ being removed), which makes the DC-located distortion happens. Additive white Gaussian noise (AWGN) is also included in the simulation channel. The simulated constellations in Fig. 3 illustrate that the proposed DC-zeroing algorithm significantly improves performance by avoiding DC-altered distortion.

Moreover, even though the DC-zeroing scheme is applied and there is no DC-altered distortion, the time-domain signal of $\hat{\mathbf{x}}_l$ is not the desired $\mathbf{s}_l$. Hence, a Hilbert filter is used to cancel the negative band of received signal, and $\hat{\mathbf{x}}_l$ becomes,

$$\mathcal{H}\{\hat{\mathbf{x}}_l\} = [x_{(l-1)N+1} \;\; x_{(l-1)N+2} \ldots x_{lN} \;\; 0 \; 0 \ldots \; 0]^{\mathrm{T}} \tag{3}$$

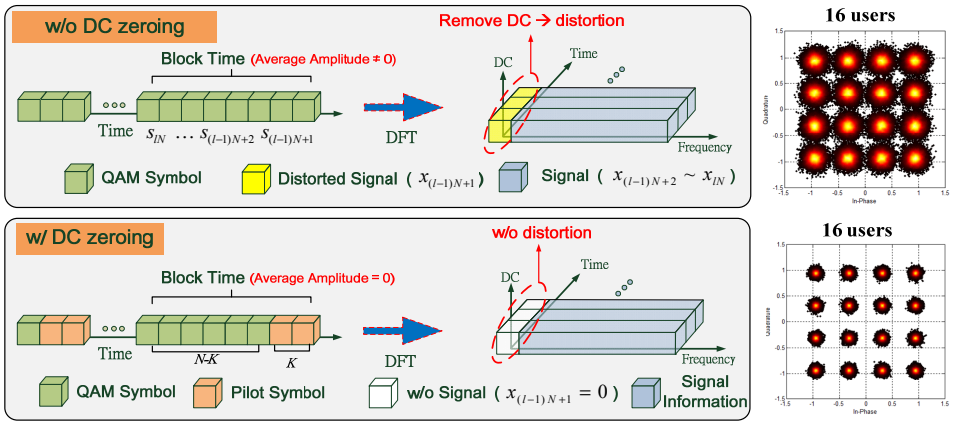

Fig. 3. Illustration of DC-zeroing algorithm and corresponding constellations.

Optics EXPRESS

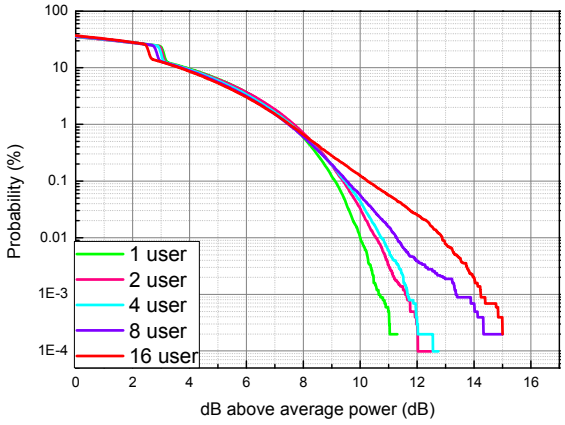

Fig. 4. PAPRs of 1~16 users with 4/32 overhead.

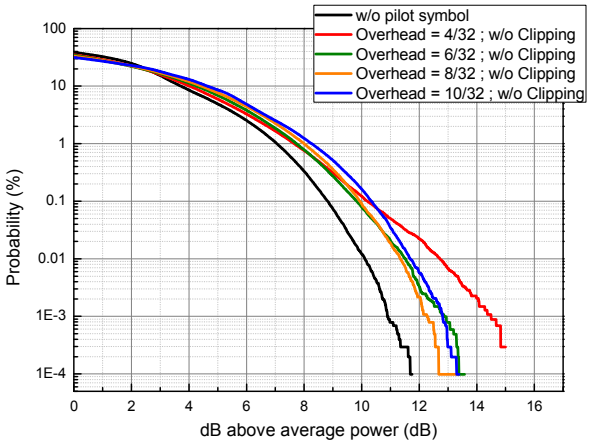

Fig. 5. PAPRs of L = 16 with 4/32–10/32 overhead.

After the Hilbert filter, the signal is down-sampled by two (i.e., removing even samples), such that the last N zeros in (3) can be removed. In other words, the down-sampled signal is the desired $\mathbf{s}_l$. To be brief, in addition to pre-processing and sub-Nyquist sampling, the application of Hilbert filter and down-sampling makes it possible for users to obtain their own vector signals in the time domain without the need for DFT and IDFT.

3. Discussion and experiment result

To investigate the PAPR of spread-OFDM using the proposed scheme, Fig. 4 shows the PAPRs with users number L of 1–16 and overhead K/N of 4/32. As the number of users increases, symbols of each block ($\mathbf{s}_l$) will be less, which increases PAPR. However, the PAPRs with L of 1–16 are almost the same at the complementary cumulative distribution function (CCDF) of 10^{-3} because only pilot symbols ($s_{(l-1)N+1} - s_{(l-1)N+K}$) of few blocks (≅1%) get high peaks but not all data symbols. Moreover, although the DC-zeroing scheme

Optics EXPRESS

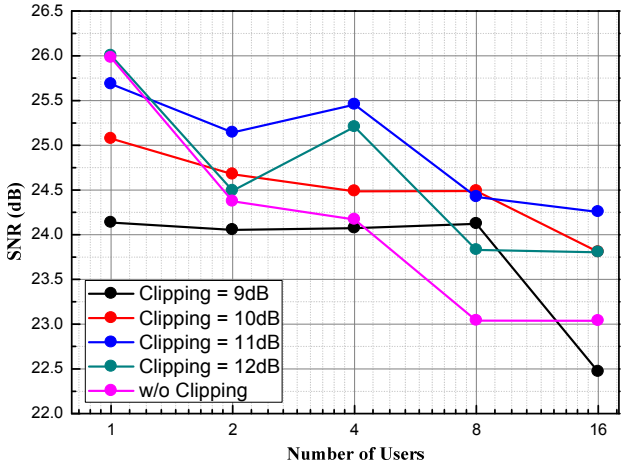

Fig. 6. SNRs of L = 1–16 with different clipping level in case of electrical BTB.

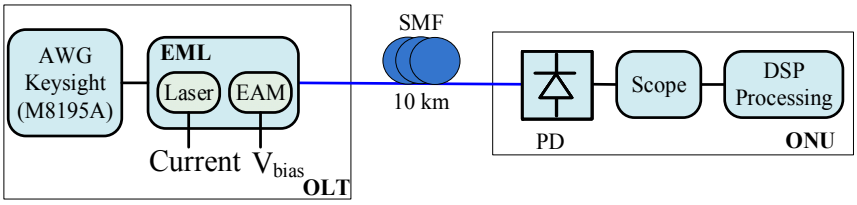

Fig. 7. Experiment setup of PON.

can effectively eliminate the issue of DC-altered distortion, the usage of pilot symbols may increase the PAPR because the sum of data amplitudes ($\sum_{n=K+1}^{N} s_{(l-1)N+n}$ in (2)) may be too high to be shared by K pilot symbols, particularly when K is small. Figure 5 shows the PAPRs of 16-user system with overhead of 4/32–10/32. Applying higher overhead can contain the high peak values, which greatly reduces the PAPRs. To achieve the balance between PAPR and overhead, clipping is used to cancel the pilot symbols which are higher than the setting PAPR level. Notably, because clipping makes the average of amplitudes no longer to be zero, DC-altered distortion cannot be completely cancelled. Since output power of ADC is limited by the highest peak value, the application of clipping is a trade-off between getting higher signal power from ADC and mitigating the DC-altered distortion. To achieve best performance, clipping level is optimized in the case of electrical back-to-back (BTB) as shown in Fig. 6. With 4/32 overhead, 11-dB clipping can achieve the best signal-to-noise power ratio (SNR) performance. Comparing the best performance of different L, however, clipping causes about 1.5-dB SNR penalty for large L (e.g. L = 16) because larger L leads to the more serious regrowth of PAPR. The overheads are set the same in different L, which makes pilot symbols with larger L are much fewer than that with small L. Hence, it is harder to share the sum of data amplitudes. To experimentally verify the proposed system, we adopt passive optical network (PON) to be the testbed (i.e. spread OFDM PON). Figure 7 illustrates the setup of experiment used to evaluate the proposed scheme. The optical transmitter was an electro-absorption modulated laser (EML). The receiver at the end of the 10-km single-mode fiber (SMF) comprised a PIN PD and an ADC. Instead of using multiple sub-Nyquist ADCs, the received signal was captured using a real-time scope at a sampling rate of 80 GSample/s. An off-line DSP was used to emulate the low SR receiving scheme. The DSP also down-sampled the received signal to multiple sub-Nyquist signals with different time delays; however, it is

Optics EXPRESS

important to note that additional signal equalization, such as frequency domain equalization (FDE), was not applied. It should also be noted that when L exceeds 1, the sampling rate of low SR ADCs was below that stipulated by the Nyquist-sampling theorem.

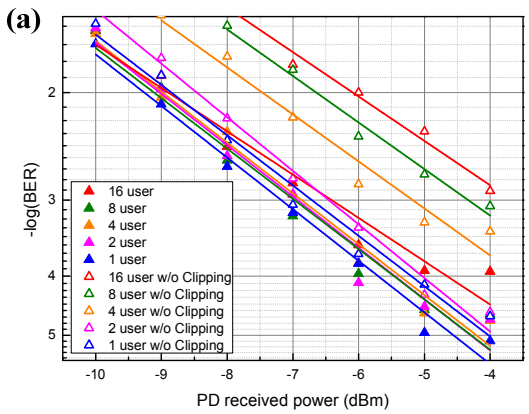

(b)

User	Sensitivity (dBm)	Improvement (dB)
16	-3.75 → 6.5	2.75
8	-4.25 → -7	2.75
4	-5.25 → -7	1.75
2	-6.5 → -7	0.5
1	-7 → -7.2	0.2

Fig. 8. (a) BER curves of 1–16 users with/without clipping in optical BTB and (b) sensitivity improvement at FEC limit of 10^{-3}.

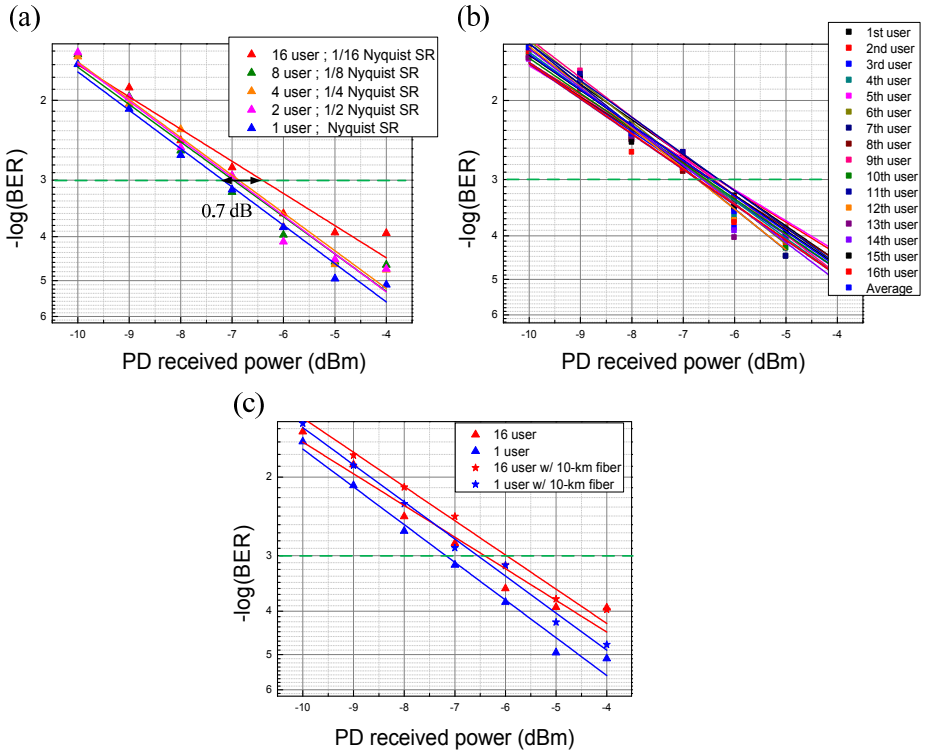

Fig. 9. (a) BER curves of 1–16 users in optical BTB, (b) respective BER curves of 16-user in optical BTB, and (c) BER curves with 10-km fiber transmission.

The spread-OFDM signal was modulated by a 16-QAM and 8 Gbauds symbol rate with corresponding Nyquist sampling rate of 16 GSample/s. In this experiment, CP was set to 1/32 and overhead was set to 4/32; therefore, the total capacity excluding CP and overhead was approximately 27.15 Gbit/s. Since the performances for different users in the multiple-user system (i.e., $L > 1$) are similar, the results in the following are the average results from 1st

Optics EXPRESS

user to L^{th} user. Figure 8(a) illustrates bit error rate (BER) curves in cases of optical BTB with clipping or not. Because the overhead is fixed at 4/32 for getting higher data rate, the PAPR regrowth is more serious. Hence, optimized clipping makes significant improvements in power budget for large L (e.g. 2.75 dB for $L = 16$).

Figure 9(a) presents the performance of the proposed scheme in optical BTB situation. The power penalty of the sub-Nyquist receiver is less than 0.5 dB at the BER of 10^{-3} when L increases from 1 to 16. Notably, when L is 16, each user just needs 1 GSample/s to recover their corresponding data. Figure 9(b) shows respective BER performances in the case of 16 users. Each user recovers its data by different sampling instants preset in pre-processing. The deviation in sensitivity from the 1st user to 16th user is quite small. These results demonstrate the efficacy of the pre-processing algorithm in the prevention of aliasing distortion beyond the Nyquist limit. Figure 9(c) presents the BER curves in cases of BTB and 10-km fiber transmission with L of 1 and 16, in which the power penalty due to 10-km fiber transmission is approximately 0.5 dB.

4. Conclusions

This paper presents a 27.15-Gbit/s multiuser spread-OFDM with DFT/IDFT-free sub-Nyquist receiver. In the proposed scheme, DFT and IDFT are not required for de-mapping aggregated signals or compensating for channel at the receiver; thus, the proposed spread-OFDM is more suitable for down-link, compared to the traditional spread-OFDM. The DC-zeroing scheme is also applied to avoid DC-altered distortion in an AC coupling system. In the experiment, the proposed scheme makes it possible to reduce the ADC sampling rate to as low as 1/16 of the Nyquist rate, with a penalty of less than 1dB at BER of 10^{-3}.